

3D Shape Classification Based on Spectral Function and MDS Mapping

Zhanqing Chen and Kai Tang*

Department of Mechanical Engineering, Hong Kong University of Science and Technology
Hong Kong, China

Abstract — This paper reports a new method for 3D shape classification. Given a 3D shape M , we first define a spectral function at every point on M that is a weighted summation of the geodesics from the point to a set of curvature-sensitive feature points on M . Based on this spectral field, a real-valued square matrix is defined that correlates the topology (the spectral field) with the geometry (the maximum geodesic) of M , and the eigen values of this matrix are then taken as the fingerprint of M . This fingerprint enjoys several favorable characteristics desired for 3D shape classification, such as high sensitivity to intrinsic features on M (because of the feature points and the correlation) and good immunity to geometric noise on M (because of the novel design of the weights and the overall integration of geodesics). As an integral part of the work, we finally apply the classical Multidimensional Scaling method to the fingerprints of the 3D shapes to be classified. In all, our classification algorithm maps 3D shapes into clusters in a Euclidean plane that possess high fidelity to intrinsic features – in both geometry and topology – of the original shapes. We demonstrate the versatility of our approach through various classification examples.

Keywords: 3D shape matching, classification, geodesic, spectral function, multidimensional scaling, feature.

◆

1. INTRODUCTION

There has been growing need of efficient techniques for search for a particular 3D shape in a database. For example, it is estimated that of all the mechanical parts today, 40% of them could be built from an existing design and another 40% could be created by modifying an existing one. When designing the shape of a new part, the designer could first make a conceptual sketch that only has certain essential topologic and geometric features of the intended part, search for the best matching objects in the company's database or some public domains on the internet, and then continue the design based on the found objects. The rapid growth of the use of internet in science and engineering also calls for a general 3D shape search tool.

A closely related problem is 3D shape classification: Given n (which is usually large) 3D shapes in certain representation, how to find an appropriate metric to measure the similarity/dissimilarity between any two of them? A toy manufacturing company could have accumulated thousands of various legacy designs of a same part, e.g., the face of a baby doll and very often it is asked that they be grouped together – based on their shapes' similarity – for human examination for the purpose of initiating a new design.

Central to 3D shape matching/classification is the extraction of salient topological and geometric features of the 3D shape and their representation in a simple form in lower dimensions. The extracted features should be intrinsic, i.e., they should be both independent of any particular surface representation and invariant to affine transformations. The representation of the features should be succinct and simple enough so that comparisons can be easily made. In addition, as more and more mesh models are being used and accumulated, the extraction algorithm ought to be insensitive to curvature noise and small undulation on the object surface. A good 3D shape

*Corresponding author. Email: mektang@ust.hk; Phone: +852 23588656

matching/classification scheme should have the following desired properties:

- (i) It is invariant under rigid-body transformations.
- (ii) It should be general, and invariant to the shape's representation – the same object, M , if given in a Boundary Representation form or a densely triangulated mesh form, the two should have identical or very close “fingerprints”.
- (iii) It should be insensitive to geometric noise and small undulations on the object's surface – this is becoming more important than before, as more and more parts are obtained by reconstructing a mesh from a point-cloud and geometric noise is inevitably generated on the final reconstructed surface due to both sampling errors and reconstructing errors.
- (iv) The algorithm should be numerically stable and the computing time should be reasonable.
- (v) It should offer a decently high classification rate.

Among various feature extraction/representation schemes, the recent Multiresolutional Reeb Graph (MRG) [1] method has drawn certain interest owing to its good immunity to geometric noise and concise graph representation. An MRG is characterized by a continuous spectral function defined on the 3D shape and a partitioning of the surface whose dual is the final feature graph. A good MRG should be one whose spectral function is not only capable of encapsulating intrinsic features of the shape but also insensitive to curvature noises, and the partitioning scheme is systematic and can be efficiently computed. However, current MRG algorithms are not able to satisfy all these requirements – they are either very sensitive to curvature noises (such as most curvature-based algorithms) or incapable of capturing curvature sensitive features (such as those purely based on geodesics).

Inspired by the idea of spectral function, in this paper we present a new spectral-function-based 3D shape classification algorithm that aims at performing better in fulfilling the aforementioned requirements. The algorithm has the following four plausible features:

- (1) On spectral function. Our spectral function is a weighted integration of the geodesic distances to a curvature-based feature set on the surface – compared to the simple form of [1], which is independent of curvature-sensitive points, ours is believed to be more potent in capturing topological and geometric features.
- (2) On immunity to noises. The mutually negating weights associated with the feature points of opposite curvature signs have been proven in our experiments to be very effective in canceling out small curvature and geometric noises on the mesh of the object.
- (3) On fingerprint extraction. We present a novel idea of partitioning the surface by its geodesic offsets that are associated with a maximum geodesic and then correlating the offset regions with the range segmentation of the spectral function. The correlation results in a square matrix whose eigen values are then taken as the fingerprint of the shape.
- (4) On the final classification scheme. We propose adopting the classical Multidimensional Scaling (MDS) method to classify 3D shapes represented by their fingerprints of (3). The MDS transforms the input fingerprints into their counterparts in a Euclidean plane whose classification is then established based on their proximities to each other.

The paper is organized as follows. We first provide a general review of the related works in 3D shape matching and classification. Section 3 then presents a detailed description of our new spectral function, followed by the description of the correlation procedure and the ensuing eigen system, in Section 4. The classical MDS and its particular application in our classification problem are given in Section 5. Finally, Section 6 presents the experimental results along with our discussion, and we conclude the paper in Section 7.

2. Background and Related Works

The existing 3D shape matching/classification algorithms can be put into several taxonomies. The taxonomy can vary, depending on the focal point and applications. Two recent surveys [2] and [3]

gave excellent reviews on them. In the following, we mainly take that from [3].

Skeleton-based methods. The most representative method of this group is the medial-axis method. Basically, assuming the object M to be a two-manifold, the medial-axis of its boundary surface is well defined and can be used to act as the fingerprint of M (cf. [4]). This medial-axis is intrinsic to M and generally is excellent in encapsulating the topology of M ; thus properties (i), (ii), and (v) are usually satisfied. The amount of the existing research work in feature extraction/representation based on medial-axes and their variances is both extensive and intensive, cf. [5, 6, 7, 8, 9, 10, 11]. Unfortunately, 3D medial-axes are known to be notoriously sensitive to small changes in geometry and their computation is tedious, time-consuming, and also numerically unstable unless uniform spatial partitioning (e.g. voxel representation) is used which further slows down the computation. As a result, except for some special and limited situations, skeleton-based methods have not been used as a practical tool.

Histogram-based methods. In this group, the fingerprint of a shape M is represented as a histogram of some local geometric measure at the sample points on M . For instance, the measure could be the Gaussian curvature at a point and the histogram counts the numbers of sample points at different Gaussian curvature levels (cf. [12]). The basic idea can also be extended to certain global measures. For example, recently Osada et al. [13] used the Euclidean distance between two random points on M as a measure and then compared any two surfaces by evaluating the distance between their corresponding statistical histograms. Since no topology is needed for constructing the histogram, such methods are usually fast and stable. On the other hand, they cannot estimate local features and their classification rates are considered to be low.

Face-based methods. These methods are more atoned to mechanical parts that are stored in some face-based format, such as Boundary Representation. There are a variety of them, such as in [14,15,16,17,18,19,20]. The general idea is to use a graph to represent the part M , where each node in the graph corresponds to a face on M with an attribute vector containing some measures of the face such as the surface area, the normal vector(s), the curvature distribution, dihedral angles with the neighboring faces, etc. They have found some success in applications in CAD/CAM. However, they are inadequate for a general 3D shape search. More critically, they violate property (ii).

MDS-based methods. Multidimensional scaling (MDS) is a family of powerful methods that map objects in higher dimensions to their counterparts in lower dimensional Euclidean spaces with the original similarity/dissimilarity respected. It has achieved marked success in some large volume data mining problems such as image understanding [21]. Recently, Elad and Kimmel [22] used the geodesics on the surface of M as the dissimilarity and applied the MDS to transform M into another (mesh) model in the 3D space. This transformation can reveal certain commonality among isometric surfaces. However, since the transformed M is still a 3D object, it is difficult to use it as an automatic tool to match against other 3D objects for classification.

Multiresolution Reeb Graph (MRG) methods. These are the more recent development in 3D shape search techniques. Basically, a continuous scalar function $\mu(\mathbf{x})$ – called the spectral function – is defined on the surface of M . The surface of M then is partitioned into a number of regions based on the range of $\mu(\mathbf{x})$, and the dual graph of this partitioning acts as the “fingerprint” of M . The spectral function is sought to capture intrinsic features of M . For example, it can be the Gaussian or mean curvature on the surface or some local surface measures. Such a locally defined spectral function however has a serious flaw: it is extremely sensitive to geometric noise, and thus severely violates criterion (iii). Recently, Higala et al. [1] proposed a spectral function based on a global measure – the $\mu(\mathbf{x})$ is the total of the geodesic distance from point \mathbf{x} to every other point on the surface. This $\mu(\mathbf{x})$ enjoys several desirable properties including (iii). However, since it completely ignores any local features (e.g., curvature), shapes of obviously distinct features may have

an identical or very similar $\mu(\mathbf{x})$. As an illustration in the 1D case, all the curves in Fig. 1 would have an identical $\mu(\mathbf{x})$, a constant, even though they “look” drastically different. For the partitioning of the surface, they gave an elaborate algorithm that builds the MRG based on merging neighboring triangles on the mesh of the surface. In their algorithm, however, important elements of the dual graph of the partitioning, such as the number of nodes and the connectivity, are critically dependent on some user- or program-decided parameters such as the range of the μ -values for a node. This strong dependency causes uncertainty on the graph and ambiguity for the ensuing graph-matching.

Finally, pertinent to spectral functions is a recent work by Reuter et al [23]. Their spectral function is actually the solution to the Laplacian eigen-value problem $\Delta\mu = -\lambda\mu$, where $\Delta\mu := \text{div}(\text{grad } \mu)$ with $\text{grad } \mu$ being the gradient and div the divergence of μ , both with respect to the (manifold) M (cf. [24]). The corresponding eigen values $0 \leq \lambda_1 \leq \lambda_2 \leq \dots \uparrow +\infty$ are then taken as the “fingerprint” of M . Notwithstanding its mathematical elegance, its biggest disadvantage is the huge computing effort – in [23] FEM was used to solve the equation $\Delta\mu = -\lambda\mu$ and only very few and simple open-mesh surfaces were tested. It is still unclear at present how this method would fare in practical 3D shape searching, in terms of both computing feasibility and actual classification effectiveness. Other important works pertinent to Laplacians include that of Belkin and Niyogi [25, 26, 27] that investigated using Laplacian eigenmaps to deal with the semi-supervised problem, whose content however is beyond the scope of this research. Shi et al. proposed a novel method of computing skeletons of robust topology for simply connected surfaces with boundary by constructing Reeb graphs from the eigenfunctions of an anisotropic Laplace-Beltrami operator [28]. Ryutarou employed an algorithm called Laplacian Eigenmaps proposed by Belkin et al. to learn a manifold spanned by shape features of 3D models in the corpus [29].

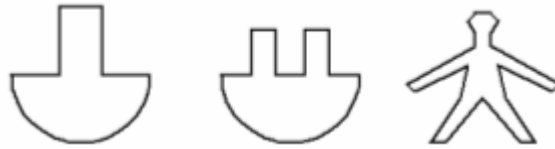


Fig. 1. All the three figures will have a constant spectral function $\mu(\mathbf{x})$ according to [1].

3. Spectral Function

Let M be a Riemannian manifold. In this work, we consider surfaces in Euclidean space that are two-manifolds with or without boundary. We emphasize that, although theoretically a 3D object is always a two-manifold without boundary, by allowing M to have boundary, our algorithm accommodates small cracks or other types of abnormality on M , which are unavoidable due to geometric noise. For two arbitrary points \mathbf{x} and \mathbf{y} on M , let the geodesic distance between them on M be denoted as $d_M(\mathbf{x}, \mathbf{y})$. Let Φ be a set of points on M to be referred to as the *feature points*. Each $\mathbf{y} \in \Phi$ is associated with a real-number weight $w(\mathbf{y})$. The feature-points-based weighted geodesic integration at an $\mathbf{x} \in M$ is defined as:

$$\mu(\mathbf{x}) = \sum_{\mathbf{y} \in \Phi} w(\mathbf{y}) d_M(\mathbf{x}, \mathbf{y}) \quad (1)$$

It is noted that the above spectral function degenerates to exactly the one used in [1], if $\Phi = M$ and all the weights are 1. It is the set Φ that we hope can better capture the intrinsic geometry and topology of M . In this work, a point $\mathbf{y} \in M$ is placed in Φ if and only if one or more of the following conditions are met:

- (a) M is not G^1 continuous at \mathbf{y} , i.e., M does not have a normal at \mathbf{y} .

- (b) The normal curvature of M is discontinuous at \mathbf{y} in some direction.
(c) $\max\{|k_1|, |k_2|\} > \sigma$, where k_1 and k_2 are the principal curvatures at \mathbf{y} , and σ is user-specified.

The weight of $\mathbf{y} \in \Phi$ is defined by:

$$w(\mathbf{y}) = \begin{cases} 1 & \text{if } M \text{ is locally convex at } \mathbf{y} \\ -1 & \text{otherwise} \end{cases} \quad (2)$$

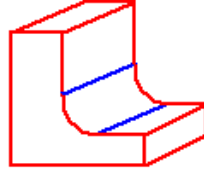


Fig. 2. A simple solid: red lines are “1” feature points and blue lines are “-1” feature points.

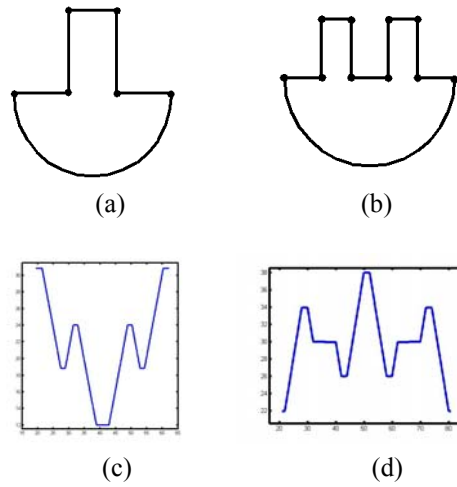


Fig. 3. Spectral curve $\mu(\mathbf{x})$: two shapes ((a) and (b)) and their respective $\mu(\mathbf{x})$ ((c) and (d)).

Fig. 2 shows a simple example of our feature set definition. We point out that M will be given as a triangular mesh, and the local convexity at an edge is decided by checking the dihedral angle of the edge. This helps overcome the difficulty of determining the local convexity at those hyperbolic points (e.g., the two arcs in Fig. 2). Fig. 3 shows two 1D examples of $\mu(\mathbf{x})$. The following observations can be made about $\mu(\mathbf{x})$.

- It is invariant under rigid body transformation.
- It is insensitive to the sampling resolution of M when it is represented as a triangular mesh, as long as the feature point set remains the same.
- It has a good immunity against geometric noise, owing to the following three reasons: (1) since the noise is usually small in magnitude, its effect on geodesic distance $d_M(\mathbf{x}, \mathbf{y})$ is tiny; (2) in many cases, because of the way the weight $w(\mathbf{y})$ is assigned, the false feature points locally cancel each other, as illustrated in Fig. 4; and (3) even if a false feature point is not canceled out, its effect on $\mu(\mathbf{x})$ is still very small as $\mu(\mathbf{x})$ is a summation (when M is a triangular mesh) whose magnitude is generally large.

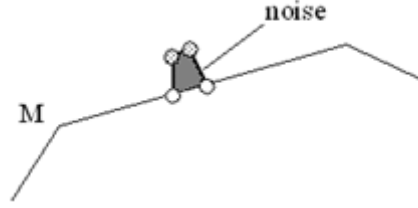


Fig. 4. The four false feature points cancel each other as two have weight “1” and the other two “-1” and the four points are close to each other.

We believe that the thus defined feature-points-based spectral function is better than simply letting $\Phi = M$ as in [1] in terms of encapsulating the geometric and topologic features of M . For instance, in the extreme case of 1D, setting $\Phi = M$ would result in a constant $\mu(\mathbf{x})$, completely ignoring the geometry of M . Another point worth noting is that, in addition to the benefit of canceling out false feature points due to noise, assigning mutually negating weight to a feature point based on its curvature sense (Eq. (2)) is clearly superior to that of using a constant weight (cf. [1]). As an example, if a constant weight is used regardless of the curvature sense, the spectral functions of the two distinctly different 2D shapes in Fig. 3(a) and (b) would look exactly the same (Fig. 5).

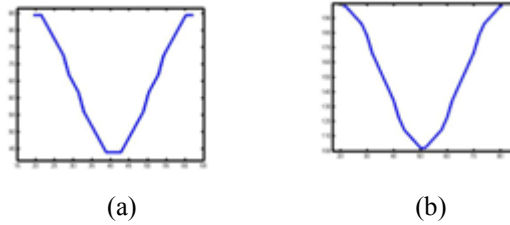


Fig 5. In the case of all “1” weight, the $\mu(\mathbf{x})$ of Fig. 3a ((a)) and Fig. 3b ((b)) respectively.

Fig. 6 displays a mechanical part and its spectral field $\mu(\mathbf{x})$. We point out that, for certain types of geometry, such as a torus, the feature set Φ may turn out to be nil. Other types of criteria for feature points can also be incorporated. For example, one might consider those points with (local) minimum or maximum absolute Gaussian curvature $|K|$. One big advantage of the proposed $\mu(\mathbf{x})$ is that the integration in Eq. (1) is point-based – the feature points are not required to form a segmentation of M . This makes their identification much easier since only local analysis is needed.

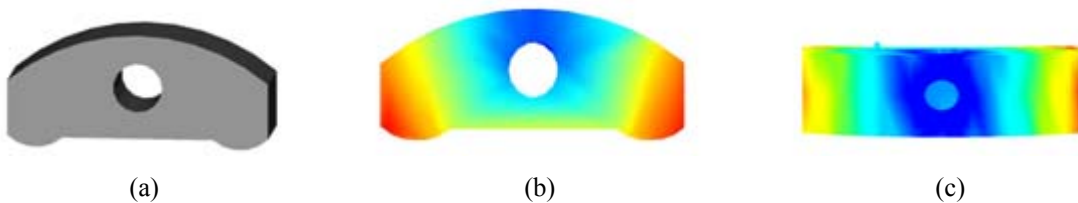


Fig. 6. A mechanical part (a) and its spectral field $\mu(\mathbf{x})$ ((b) and (c)).

About the geodesic calculation, since this computation is carried out heavily (Eq. (1)), its speed is paramount. Rather than relying on exact but very slow geodesic calculation (such as the MMP algorithm in [30]), we adopted in principle the fast approximate geodesic algorithm of [31]. When implementing this algorithm, we made several important modifications in order to accommodate geometric abnormalities in a mesh. The original algorithm of [31] strictly requires the mesh to be a two-manifold without boundary. For us, however, boundary edges (Fig. 7(a)) and even non-manifoldness (Fig. 7(b)) must be allowed. To suit these needs, we devised a non-manifold

representation for meshes and broadened the window propagation in the algorithm of [31]. In addition, as geometric degeneracy is unavoidable during the computation, we also incorporated the degeneracy handling scheme as given in [32].

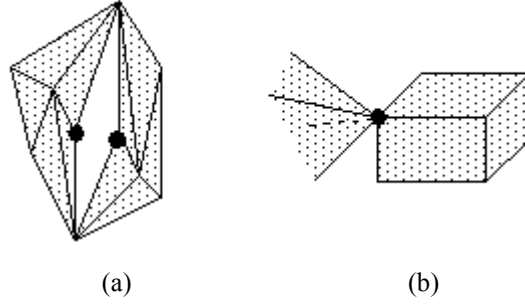


Fig. 7. Abnormalities in a mesh due to geometric noises.

4. Characteristic Matrix and Eigen Values

Once the spectral field $\mu(\mathbf{x})$ on M is obtained, our next task is to extract its “fingerprint”. In other words, we need to find a suitable transformation that converts $\mu(\mathbf{x})$, which is of infinite dimensions, into an entity of lower dimensions – ideally a point in \mathbf{R}^m for some small m . Originally we tried the idea of partitioning M according to the range of $\mu(\mathbf{x})$ and then using the dual graph of the segmentation as the fingerprints, as suggested in [1]. Unfortunately, our experiences with this approach were not satisfactory. First, the final fingerprint is a non-planar graph whose structure crucially depends on various user-specified parameters during the partitioning, which makes it less dependable as an intrinsic embodiment of M , letting alone the difficulty itself of faithfully comparing two non-planar graphs. Second, and more critically from practical point of view, since inevitably the field $\mu(\mathbf{x})$ has to be discretized by its values at sample points on M , the partitioning must be performed in this discrete domain, which has been found to be inordinately susceptible to numerical instability. Instead, we propose a scheme based on the idea of correlating the geometry with the topology and the eigenization of the correlation result.

First, let us define a *spine* S on M to be a maximum geodesic on M , i.e., S has the maximum length among all the geodesics on M . M might have several maximum geodesics, of which any one can serve as S . Let p_s and p_t denote the two end points of S , and m be a fixed and positive integer. Setting $\Delta_g = d_M(p_s, p_t)/m$, the *geodesic offset set* (GOS) G_i , for $i \in \{1, 2, \dots, m\}$, is defined as:

$$G_i = \{\mathbf{x} \in M: (i-1) \cdot \Delta_g < d_M(p_s, \mathbf{x}) \leq i \cdot \Delta_g\}. \quad (3)$$

The m G_i form a “strip”-like partitioning on M – obviously, if M is planar, G_i is a con-centric circular band with p_s being the center. It is imperative to note that this partitioning is never explicitly constructed. As M is essentially represented by the sample points (hereafter we will use V to symbolize the set of these sample points), set G_i can be easily found by examining the sample points with the required geodesic distances to p_s , which are already available after $\mu(\mathbf{x})$ is calculated.

Next, the G_i is correlated with $\mu(\mathbf{x})$. Specifically, letting $\Delta_\mu = (\mu_{\max} - \mu_{\min})/m$, where μ_{\max} and μ_{\min} are the maximum and minimum $\mu(\mathbf{x})$ respectively, we define the $m \times m$ *characteristic matrix* C_M of M as:

$$C_M[i, j] = \frac{\|\{\mathbf{p} \in G_i : (j-1) \cdot \Delta_\mu < \mu(\mathbf{p}) \leq j \cdot \Delta_\mu\}\|}{\|V\|}, \quad (i, j) \in [1, m] \times [1, m], \quad (4)$$

where $|\cdot|$ stands for the number of elements in the (finite) set. The purpose of the denominator $|\mathbb{V}|$ is obvious: it normalizes the counting and thus averts the problem caused by different number of sample points on different M . Note the partition-of-unit property of C_M : $\sum \sum C_M [i, j] = 1$.

C_M is already a dimension reduction – it reduces an infinitely dimensional $\mu(\mathbf{x})$ to \mathbf{R}^{m^2} . Nonetheless, we pursue further by extracting the eigen values of matrix C_M , out of two considerations. For one, using a matrix as the fingerprint is still cumbersome and less effective, even more so for our classification task. The other owes to the recent research results in computer vision (cf. [24]) that the eigen values/vectors in general are better in capturing principal components of a density matrix, not mentioning a significant dimension reduction from m^2 to m or less. Therefore, as the final step of our fingerprint extraction, we compute the eigen values of C_M and sort them in decreasing order according to their absolute magnitudes:

$$|\lambda_1| \geq |\lambda_2| \geq |\lambda_3| \geq \dots \geq |\lambda_k| \geq 0, \quad k \leq m.$$

This ordered list will be referred to as the *spectral eigen sequence* (SES) of M and denoted as $\sigma(M)$. In Fig. 8, we show the SES's of three mechanical parts (eccentric cams), which clearly reveal the similarity and dissimilarity among the three.

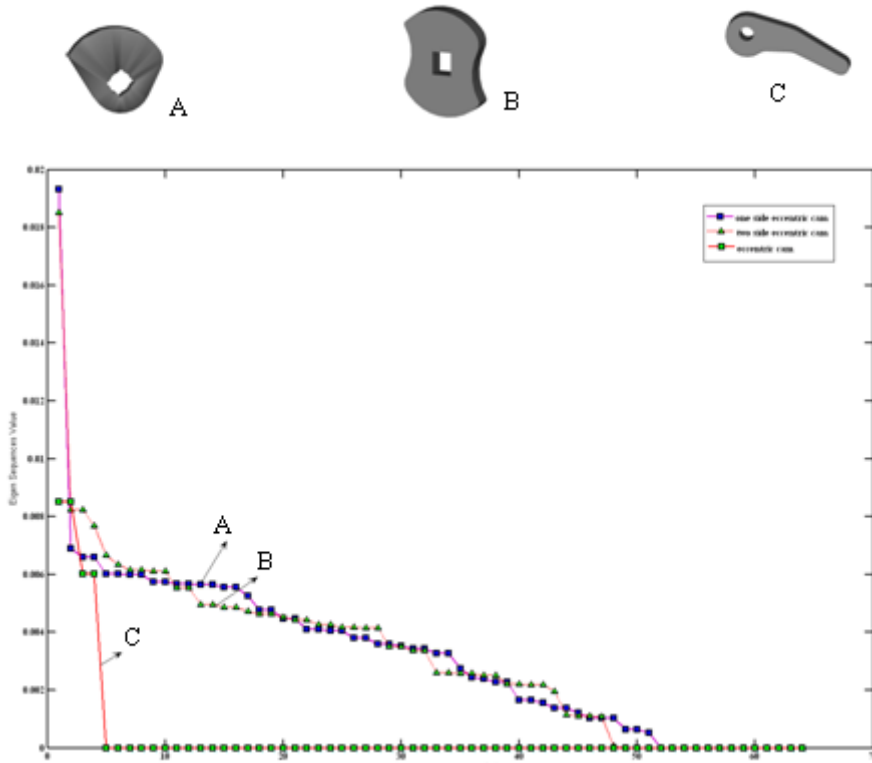


Fig. 8. Spectral eigen sequences of three eccentric cams.

5. MDS-based Classification

Now that a 3D shape M is uniquely represented by its spectral eigen sequence $\sigma(M)$, which is a point in an embedded subspace of \mathbf{R}^k , our final mission is to choose a comparison method whose assessment of the similarity/dissimilarity between $\sigma(M_1)$ and $\sigma(M_2)$ also faithfully reflects that between M_1 and M_2 themselves. The naïve L_2 measure between $\sigma(M_1)$ and $\sigma(M_2)$ – i.e., the Euclidean distance in \mathbf{R}^k – should be ruled out at once, as it is well known that this measure is

usually extremely poor in reflecting the true similarity or dissimilarity of the original 3D shapes.

Among a number of options, the Multidimensional Scaling (MDS) (cf. [33, 34, 35]) method is eventually adopted by us. This method has been proven to be a powerful tool for revealing principal components among large sets of data items, especially in various statistics applications. Recently, it has found encouraging results in 3D shape processing such as texture mapping [36] and bending invariant signatures for surfaces [22]. The goal of MDS algorithms is exactly what we wanted here: to map an entity in higher dimensions to a point in a lower dimensional Euclidean space \mathbf{R}^d (in our case $d = 2$) while trying to preserve the original similarity/dissimilarity as much as possible. Specifically, in our setting, given n spectral eigen sequences $\sigma(M_1), \sigma(M_2), \dots, \sigma(M_n)$, the result of an MDS is a mapping $\sigma(M_i) \rightarrow \mathbf{x}_i \in \mathbf{R}^d$ such that the following stress function is minimized:

$$E = \frac{\sum_{i < j} w_{ij} (\delta_{ij} - d_{ij})^2}{\sum_{i < j} \delta_{ij}^2}, \quad (5)$$

where δ_{ij} is the dissimilarity measure between $\sigma(M_i)$ and $\sigma(M_j)$, d_{ij} is the Euclidean distance between \mathbf{x}_i and \mathbf{x}_j , and w_{ij} are some weighting coefficients. In our current solution, δ_{ij} is set to be the L_2 Euclidean distance between $\sigma(M_i)$ and $\sigma(M_j)$, i.e.,

$$\delta_{ij} = \left(\sum_{l=1}^k (\lambda_{il} - \lambda_{jl})^2 \right)^{1/2}, \quad \text{with } \sigma(M_i) = [\lambda_{i1}, \lambda_{i2}, \dots, \lambda_{ik}]^T \text{ and } \sigma(M_j) = [\lambda_{j1}, \lambda_{j2}, \dots, \lambda_{jk}]^T.$$

There are several known algorithmic techniques for the minimization of (5), of which the classical MDS method is considered to be an excellent algebraic approach. Let $\mathbf{X} = [\mathbf{x}_1, \mathbf{x}_2, \dots, \mathbf{x}_n]^T$ be the set of n d -dimensional points to be found, and define the inner product matrix $\mathbf{B} = \mathbf{X}\mathbf{X}^T$. Under the classical MDS, the \mathbf{B} corresponding to the best \mathbf{X} should be equal to $-\frac{1}{2}\mathbf{J}[\delta_{ij}]\mathbf{J}$, with $\mathbf{J} = \mathbf{I} - \frac{1}{n}\mathbf{I}\mathbf{I}^T$ and $\mathbf{I}_{1 \times n} = [1, 1, \dots, 1]^T$. As the inner product matrix \mathbf{B} is symmetric, positive semi-definite, and of rank d , it has d nonnegative eigenvalues and $n - d$ zero eigenvalues. \mathbf{X} then is set to be $[\mathbf{V}_1 \ \mathbf{V}_2 \ \dots \ \mathbf{V}_d]_{n \times d}$, with \mathbf{V}_i ($1 \leq i \leq d$) being the d eigenvectors of the nonnegative eigenvalues. Strictly speaking, the classical MDS minimizes a variance of the E in (5), but not E itself. Nonetheless, it is chosen by us because of its faster running time ($O(n^2)$).

6. Experimental Results and Discussion

A preliminary version of our 3D shape classification algorithm has been implemented and tried on a number of mechanical parts. All the tested parts are downloaded from the internet in the standard STL format, which is a popular triangular mesh representation for online data transmission. Many of them are found to have various kinds of abnormality and geometric or topological inconsistency such as small cracks, overlapping of triangular faces, misplaced or hung faces, etc. These models are directly input to our algorithm without any repair or modification. In all the tests, the dimension d of the MDS analysis is 2.

In the first test, shown in Fig. 9, the final MDS result correctly captures the geometric similarity/dissimilarity among five eccentric cams, of which three (and their SES's) are already shown in Fig. 8. To gauge the performance of the proposed algorithm in the occurrence of geometric noise and scaling, two more cams (colored red in the figure) are added to the group, one with a small ‘‘bump’’ acting as a noise on a flat face, and the other is similar to one of the three in geometry but scaled down in volume by half. It is worth noting that, in the noise case, for better il-

illustration, the height of the “bump” was purposely made comparable to the size of the part. In reality, geometric noises usually have extremely small magnitudes and hence, conceivably, the two involved cams would be much closer in Fig. 9 if the “bump” were chopped in half.

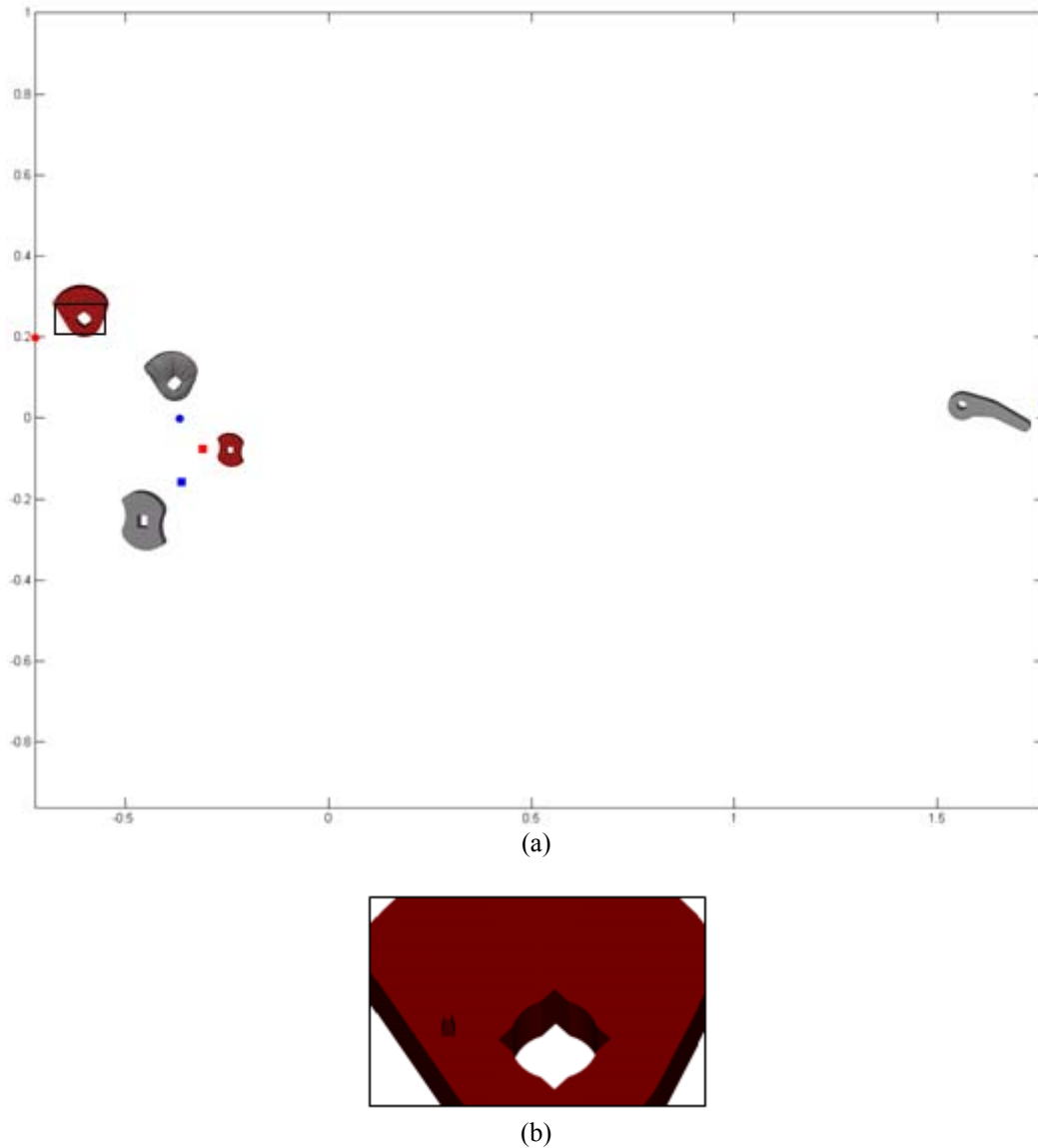


Fig. 9. The final MDS result of five eccentric cams (a), (b) is the zoomed view of one cam with noise.

Fig. 10 demonstrates the second test, on seven tables. The tables are different from each other in geometric shape (of both the legs and the top) and the number of legs. The MDS result clearly distinguishes the single two-leg table (top) from the rest. To the rest, the three four-leg tables are placed in the left, while the remaining three three-leg tables are all crowded to the lower-right corner. It is quite interesting to notice the different placements of the two three-leg tables – both with a square top but of different geometry of legs (one round and one square) – and yet their correct proximity with the other three-leg table with a round top.

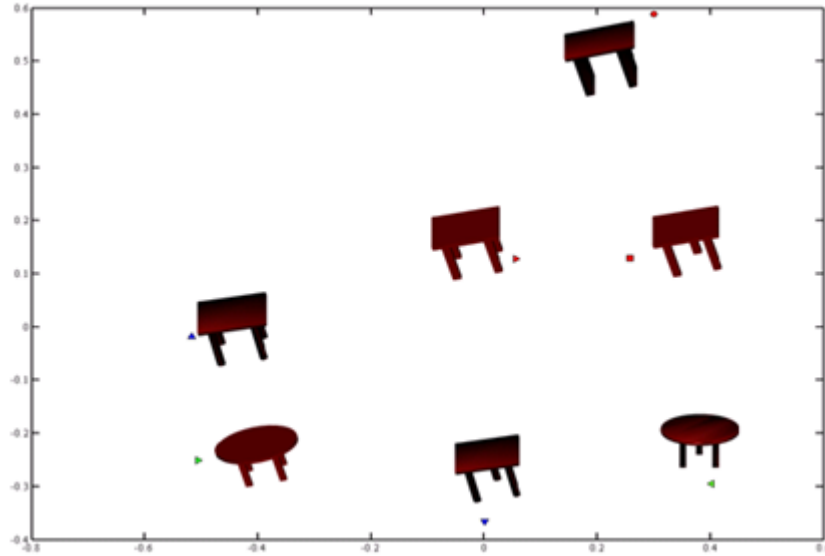
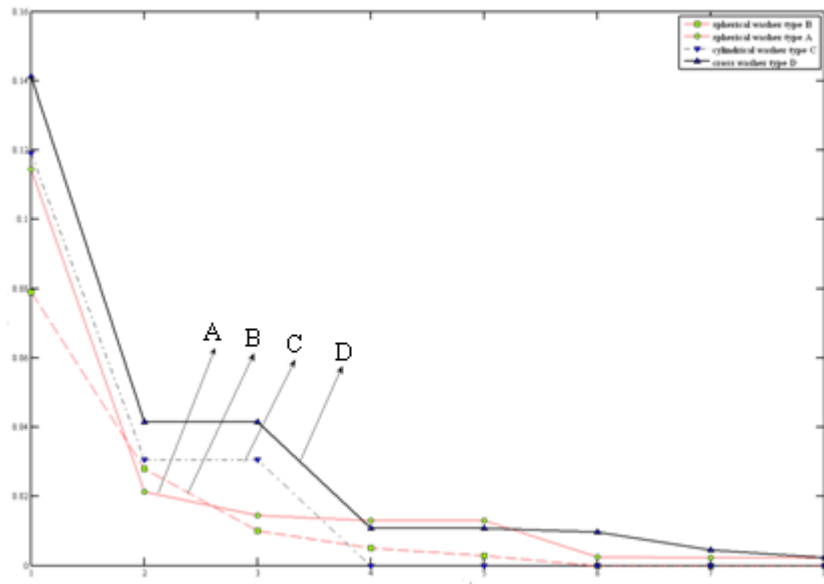


Fig. 10. The final MDS classification result of seven tables.

The third test is on four mechanical parts – washers, and the classification results are given in Fig. 11 (see also Table 1 for their labeling). It is worth pointing out that the absolute distance d_{ij} in Eq. (5) is not important – it is the relative distance that matters the most. Refer to the MDS result in Fig. 11(b). The cross type washer D, due to its more complex geometry, lies farther away from the other three. The two spherical type washers A and B have opposite directions of arc planes, which are separated by a cylindrical type washer C that has a flat base plane. The washer C can be viewed as a transition between A and B. We emphasize that the L_2 distance between the spectral eigen sequences (Fig. 11(a)) alone would never be able to provide this much rich information.



(a)

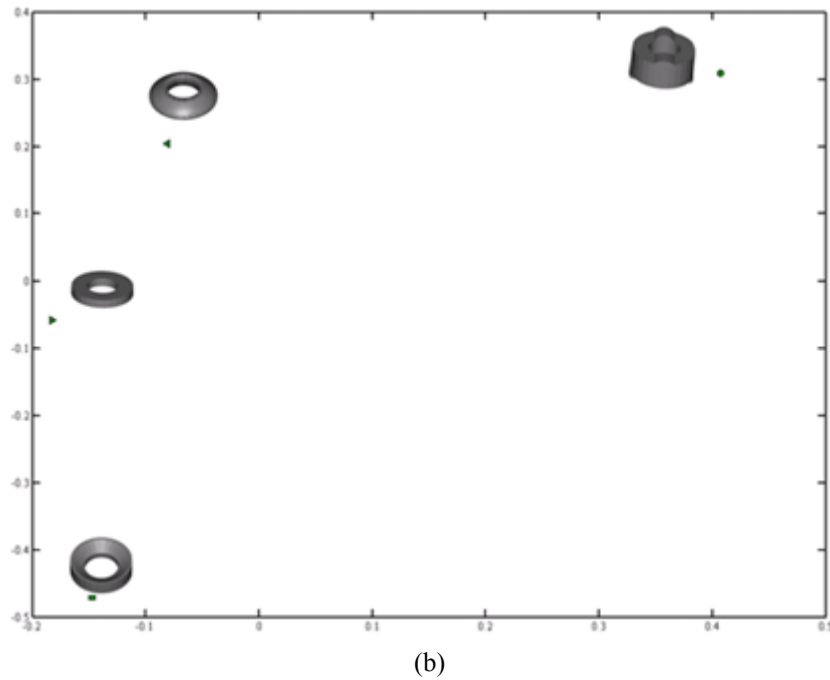









Fig. 11. Classification of four washers: (a) their SES's, and (b) the MDS result.

The final test is the classification of a library of a total of 14 fixtures (Table 1), of which some are already tested separately in the first and third test. The final classification result is shown in Fig. 12. Several plausible observations can be made. For example, the absolute distance d_{ij} this time is much smaller among the washers as compared to the case when they are classified in isolation (Fig. 11), and this time they are all placed in a tight cluster away from the rest of fixtures. The same is true for the three eccentric cams (referring to Fig. 9): this time, the arm type cam is much closer to the other two cams; and yet it is also in close proximity to those clamps (U-shaped and bidirectional) because of its geometric similarity to them. We conclude by stating the fact that, of the three arc-shaped clamps, two have genus 2 (with an extra but very small through hole) while one has only genus 1, but they are all placed, correctly, close to each other in Fig. 12. The situation would conceivably change if this tiny through hole is enlarged.

U-shaped clamp	Type A	
	Type B	
Eccentric cam	One side	
	Double side	
	Arm type	
Arc-shaped clamp	Type A	
	Type B	








	Type C	
Washer	Spherical type A	
	Spherical type B	
	Cylindrical type C	
	Cross type D	
Bidirectional clamp	Type A	
	Type B	

Table 1. Fourteen mechanical fixtures.

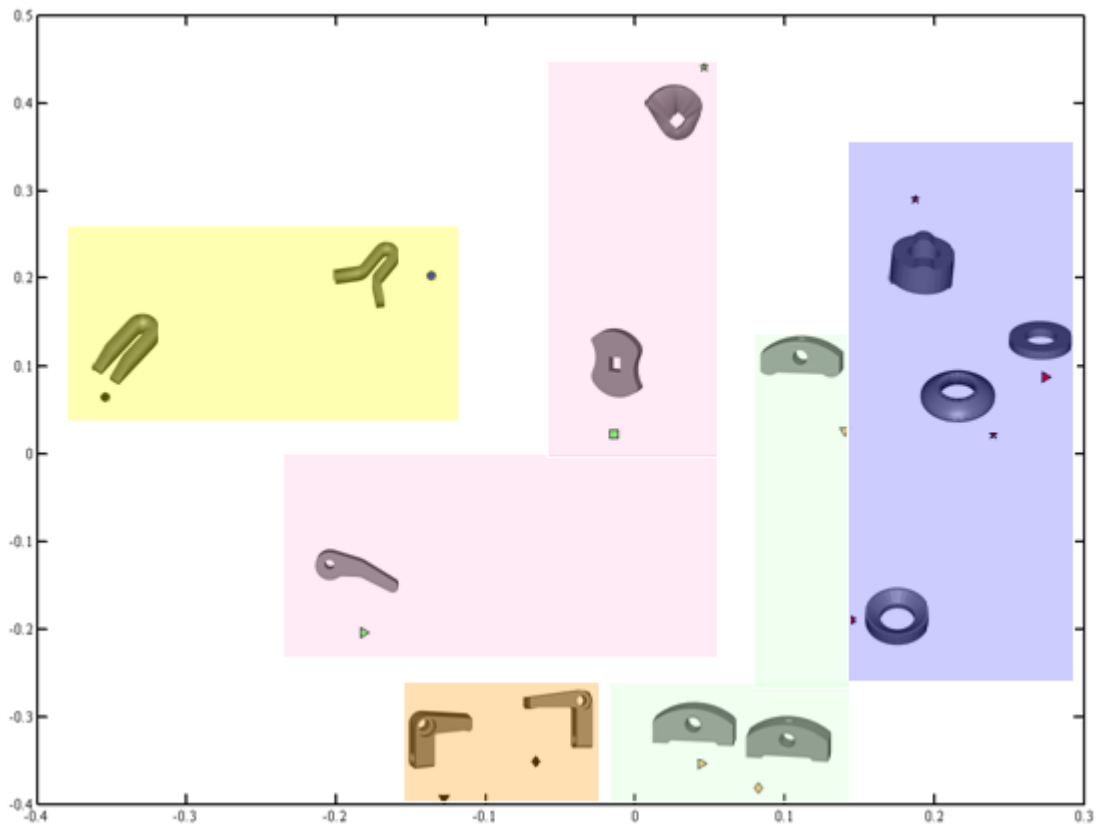


Fig. 12. The MDS classification result of the fixtures from Table 1.

7. Conclusion and Future Research

We have presented a 3D shape classification algorithm with a primary goal of attaining better ability of capturing intrinsic features (both geometric and topological) of the 3D shape while at the same time possessing high immunity against geometric or topological noises on the shape. Towards this goal, we introduced a feature-points dependent spectral function defined on the shape to encapsulate the intrinsic features of the shape, whose ability of recognizing geometric features is enhanced by its dependency on the geodesic distances from the point to the feature points, whereas the integral nature of the spectral function plus the mutually negating weights associated with the feature points of opposite curvature signs help significantly reduce its sensitivity to the geometric noises on the shape. We next gave a novel transformation based on the maximum geodesic and segmentation of the spectral function that maps the spectral function on the shape to a real-valued square matrix of small size, whose eigen values are then taken as the fingerprint of the shape. Finally, for the classification task, we proposed applying the classical MDS to the thus defined fingerprints of the 3D shapes. The entire algorithm exhibits good numerical stability – since no any explicit segmentation is constructed on the shape – and it is independent of the representation of the 3D shape. The preliminary experiments conducted by us have shown that the proposed algorithm demonstrates a certain efficacy in recognizing salient geometric and topological features on a 3D shape and a respectable classification rate for the shapes tested.

The work reported however is only preliminary and incomplete, and more tests are needed to verify the effectiveness and versatility of the proposed algorithm, including examples in more sculptured and geometrically more complex surfaces. There are several key issues remaining unanswered that call for further investigation. One is the definition of feature points. In our current experiments, a feature point is easy to define and identify – it is where G^1 continuity breaks down or principal curvatures become discontinuous, as most of the tested examples are mechanical parts. More criteria for feature points and their effect have to be studied, so to cater to surfaces that are geometrically more complex. Another is the (non-explicit) partitioning of the surface (Eq. (3)). In this work, this partitioning is based on geodesic offset and is completely independent of the spectral field which though encapsulates both geometric and topological information. A more reasonable approach is to also consider the spectral field, for example, at certain critical points where the spectral function attains extremum values. In addition, the segmentation size m (for Eq. (3) and (4)) currently is arbitrarily set and its influence on the final classification result is not clear at present. Finally, some popular data mining techniques other than the MDS, e.g., the Principal Component Analysis, deserve to be tried.

Acknowledgement

This work is partially supported by Hong Kong research grant RGC 07/08 EG.620307.

References

- [1] M. Hilaga, Y. Shinagawa, T. Kohmura, T. Kunii, “Topology Matching for Fully Automatic Similarity Estimate of 3D Shapes,” SIGGRAPH (2001), 203-212.
- [2] T. Funkhouser, P. Min, M. Kazhdan, J. Chen, A. Halderman, A. Dobkin, D. Jacobs, “A search engine for 3D models”, ACM Transaction on Graphics (2003) 22(1), 83-105.
- [3] N. Iyer, S. Jayanti, K. Lou, Y. Kalyanaraman, K. Ramani, “Three-dimensional shape searching: state-of-the-art review and future trends”, Computer-Aided Design (2005) 37(5), 509-530.
- [4] H. Sundar, D. Silver, N. Gagvani, S. Dickinson, “Skeleton based shape matching and retrieval”, Proc. of Shape Modeling and Applications (2003), Seoul, Korea.
- [5] T. Sebastian, P. Klein, and B. Kimia. “Recognition of shapes by editing shock graphs”. In IEEE International Conference on Computer Vision, pages 755–762, 2001.
- [6] L. G. Shapiro and R. M. Haralick. “Structural descriptions and inexact matching”. IEEE Transactions on Pattern Analysis and Machine Intelligence, 3:504–519, 1981.

- [7] A. Shokoufandeh, S. Dickinson, C. Jonsson, L. Bretzner, and T. Lindeberg. "On the representation and matching of qualitative shape at multiple scales". In Proceedings, 7th European Conference on Computer Vision, volume 3, pages 759–775, 2002.
- [8] K. Siddiqi, A. Shokoufandeh, S. Dickinson, and S. Zucker. "Shock graphs and shape matching". *International Journal of Computer Vision*, 30:1–24, 1999.
- [9] Oscar Kin-Chung Au, Chiew-Lan Tai, Hung-Kuo Chu, Daniel Cohen-Or, Tong-Yee Lee "Skeleton Extraction by Mesh Contraction" *ACM Transaction on Graphics (Proceedings of SIGGRAPH 2008)*
- [10] Andrei Sharf, "On-the-fly Curve-skeleton Computation for 3D Shapes" *EUROGRAPHICS 2007*, Volume 26 (2007), Number 3
- [11] Martin Styner, "Automatic and Robust Computation of 3D Medial Models Incorporating Object Variability", *International Journal of Computer Vision* 55(2/3), 107–122, 2003
- [12] H. Yamauchi, S. Gumbold, R. Zayer, Hans-Peter Seidel, "Mesh segmentation driven by Gaussian curvature," *Visual Computer* (2005) 21, 659-668.
- [13] R. Osada, T. Funkhouser, B. Chazelle, D. Dobkin, "Matching 3D models with shape distribution", *Int. Conf. on Shape Modeling and Applications* (2001), 154-166.
- [14] A. Cardone, S.K. Gupta, "Similarity assessment based on face alignment using attributed vectors", *CAD&Applications* (2006), 5(5), 645-654.
- [15] M. EI-Mehalawi, R. Miller, "A database system of mechanical components based on geometric and topological similarity. Part I: representation", *Computer-Aided Design* (2003), 35, 83-94.
- [16] M. EI-Mehalawi, R. Miller, "A database system of mechanical components based on geometric and topological similarity. Part II: indexing, retrieval, matching, and similarity assessment", *Computer-Aided Design* (2003), 35, 95-105.
- [17] S. Gao, J. Shah, "Automatic recognition of interacting machining features based on minimal condition subgraph", *Computer-Aided Design* (1998), 30(9), 727-739.
- [18] D. McWherter, M. Peabody, W.C. Regli, A. Shokoufandeh, "Solid model database: techniques and empirical results", *ASME J. Comput Info Sci. Eng.* (2001), 1(4), 300-310.
- [19] K. Tang and T. Woo, "Algorithmic aspects of Alternating Sum of Volumes: Part I. Data Structure and Difference Operation", *Computer-Aided Design* (1991) 23(5).
- [20] K. Tang and T. Woo, "Algorithmic aspects of Alternating Sum of Volumes: Part II. Non-convergence and its Remedy", *Computer-Aided Design* (1991) 23(6).
- [21] J. Tenenbaum, V. Silva, J. Lanford, "A Global Geometric Framework for Nonlinear Dimensionality Reduction," *Science* (2000) 290, 2319 – 2323.
- [22] A. Elad and R. Kimmel, "On Bending Invariant Signatures for Surfaces," *IEEE Trans. on Pattern Analysis and Machine Learning* (2003) 25, 1285-1295.
- [23] M. Reuter, F.-E. Wolter, N. Peinecke, "Laplace-spectra as fingerprints for shape matching", *Proc. of ACM Symposium on Solid and Physical Modeling* (2005), 101-106.
- [24] M. Belkin and P. Niyogi, "Laplacian Eigenmaps for Dimensionality Reduction and Data Representation," *Neural Computations* (2003) 15, 1373-1396.
- [25] M. Belkin, P. Niyogi, "Manifold Regularization: a Geometric Framework for Learning from Labeled and Unlabeled Examples", *Journal of Machine Learning Research*, 7(Nov):2399-2434, 2006.
- [26] M. Belkin, P. Niyogi, "Semi-supervised Learning on Riemannian Manifolds", *Machine Learning*, 56, Invited, special Issue on Clustering, 209-239, 2004.
- [27] M. Belkin, P. Niyogi, "Laplacian Eigenmaps for Dimensionality Reduction and Data Representation", *Neural Computation*, June 2003; 15 (6):1373-1396.
- [28] Yonggang Shi Rongjie Lai Krishna, S, "Anisotropic Laplace-Beltrami eigenmaps: Bridging Reeb graphs and skeletons", *Computer Vision and Pattern Recognition Workshops, 2008. CVPRW '08. IEEE Computer Society Conference on*
- [29] Ryutarou Ohbuchi, Jun Kobayashi, "Unsupervised Learning from a Corpus for Shape-Based 3D Model Retrieval", accepted, *ACM MIR 2006*, Santa Barbara, CA, U.S.A., Oct. 2006
- [30] J.B. Mitchell, D. Mount, and C. Papadimitriou, "The discrete geodesic problem", *SIAM J. Comput.* 16(4), (1987), 647-668.
- [31] V. Surazhsky, T. Surazhsky, D. Kirsanov, S. Gortler, and H. Hoppe, "Fast exact and approximate geodesics on meshes", *ACM SIGGRAPH* (2005), 553-560.
- [32] Yong-Jin Liu, Qian-Yi Zhou, Shi-Min Hu, "Handling degenerate cases in exact geodesic computation on triangle meshes," *The Visual Computer* 23(9-11): 661-668 (2007)
- [33] I. Borg and P. Groenen, *Modern Multidimensional Scaling – Theory and Applications*, Springer, 1997.
- [34] M.A.A. Cox and T.F. Cox, *Multidimensional Scaling*, Chapman and Hall, 1994.
- [35] J.B. Kruskal and M. Wish, *Multidimensional Scaling*, Sage, 1978.

[36] G. Zigelman, R. Kimmel, and N. Kiryati, "Texture Mapping Using Surface Flattening via MDS", *IEEE Trans. on Visualization and Computer Graphics* (2002) 8(2), 198-207.